Optimization of the PM-EDM Process Parameters for Ti-35Nb-7Zr-5Ta Bio Alloy

Ahmed Rabeea Hayyawi
Materials Engineering College, Metallurgical Engineering Department, University of Babylon, Iraq
ahmed.hayyawi.math45@student.uobabylon.edu.iq

Haydar Al-Ethari
Materials Engineering College, Metallurgical Engineering Department, University of Babylon, Iraq
dr.eng.alethri@uobabylon.edu.iq

Ali Hubi Haleem
Materials Engineering College, Metallurgical Engineering Department, University of Babylon, Iraq
mat.ali.hobi@uobabylon.edu.iq

Received: 31 December 2023 | Revised: 26 January 2024 | Accepted: 28 January 2024

 DOI: https://doi.org/10.48084/etasr.6845

ABSTRACT

Powder-Mixed Electrical Discharge Machining (PM-EDM) is one of the latest advancements in EDM process capability augmentation. This procedure involves effectively mixing a suitable material in fine powder form with the dielectric fluid. The dielectric fluid's breakdown properties are enhanced by the additional powder. The objective of the present research is to machine the Ti-35Nb-7Zr-5Ta alloy prepared by powder metallurgy and study the influence of process parameters, such as peak current, pulse-on time, pulse-off time, powder type (Ag, Si, Ag+Si), and powder concentration. The metal removal rate and SR represent the response parameters. The Taguchi approach was followed to design the experiments. The five-factor three-level design was chosen to use the Taguchi L27 orthogonal array. It was found that the addition of Ag, Si, or Ag+Si powders to the dielectric fluid enhanced the metal removal rate and the surface finish for this alloy. The addition of Ag powder to the dielectric fluid gave a higher Material Removal Rate (MRR) and a lower SR compared to Si or Ag+Si powders. Powder concentration and pulse current are the most effective parameters on MRR and SR followed by powder type, pulse-on, and pulse-off. The maximum Grey Relational Grade (GRG) exists at (I=5 A, T_{on}=9 µs, T_{off}=37 µs, P_T=Ag, P_C=20 g/L). These are the optimal conditions for PM-EDM of the Ti-35Nb-7Zr-5Ta alloy that give maximum MRR with minimum SR.

Keywords-TNZT alloy; PM-EDM; MRR; SR; optimization; GRA

I. INTRODUCTION

The final products of machining operations have very high surface quality and precision. Cutting tools used in conventional machining have to be stronger than the material of the workpiece [1, 2]. Certain materials, such as super alloys, titanium alloys, and stainless steel, are challenging to manufacture with conventional machining techniques. To prevent production from being hindered, better cutting tool materials have to be developed [3]. Utilizing materials that are challenging to cut sparked initiatives that eventually resulted in the development of unconventional machining techniques which are now widely implemented in modern industrial sectors. The hardness of the cutting tools is irrelevant because a wide range of metallic and nonmetallic materials can be machined adopting Non Traditional Machining Processes (NTMPs), many of which involve no physical contact between the workpiece and the tool [4]. Electrical Discharge Machining (EDM) is one of the most popular NTMPs employed to create complex shapes within the parts and assemblies in the manufacturing industry [5, 6]. Through a sequence of discrete electrical discharges between the electrode and the workpiece submerged in a dielectric fluid, the EDM technique transforms electrical energy into thermal energy [7]. Nevertheless, it has several drawbacks, including inadequate surface quality and limited machining efficiency. In order to get around these restrictions, a lot of work has been devoted into creating EDM systems with high MRR, high accuracy, and high precision without significantly changing their fundamental design. As a result of these initiatives, planetary motion is applied to a tool or workpiece by electrode rotation, electrode orbiting, applications of ultrasonic vibrations, and Powder-Mixed Electrical Discharge Machining (PM-EDM) [8], which is one of the newest developments for improving the EDM process capabilities. This procedure involves properly mixing a suitable material in fine powder form with the dielectric fluid. The dielectric fluid's breakdown properties are enhanced by the added powder. The spark gap distance between the electrode

and the workpiece grows when the insulating strength of the breakdown properties for the dielectric fluid lowers. Debris flushing is uniform when the spark gap is larger. This leads to a significantly more steady process, which enhances surface finish and Material Removal Rate (MRR) [9]. The particles of the added powder approach one another beneath the sparking region and are organized into patterns resembling chains. The direction of the current flow is where the powder particles interlock. The discharge gap between the electrodes is bridged in part by the chain creation. The bridging action causes the dielectric fluid's insulating strength to drop, which makes a short circuit easy to occur. Therefore, the gap explodes prematurely, and "series discharge" beneath the electrode region begins. The rate of material removal rises as an outcome of a discharge's rapid sparking, which accelerates erosion from the workpiece surface [10].

Authors in [11] investigated the surface characteristics of the PM-EDM process using Al_2O_3 and SiC abrasive powder added to the dielectric fluid for the Ti6Al4V alloy. The findings of the experiment show that the variables which most significantly affect MRR, Tool Wear Rate (TWR), and surface finish are discharge current (I_P) and powder concentration (P_C). The lowest possible values of TWR and Surface Roughness (SR) are attained at I_P = 06 A, T_{ON} = 05 µs, T_{OFF} = 96 µs, and P_C = 0.50 g/L. Authors in [12] examined the impact of incorporating Si powder into the EDM dielectric liquid on the machining properties of AISI D2, a high-carbon, high-chrome die steel. According to the ANOVA study, out of all the factors, peak current and powder concentration had the largest percentage contributions to MRR. The results of the confirmation run indicated that when AISI D2 surfaces were machined by Si powder mixed EDM, the settings of peak current at a high level (16 A), pulse-on time at a medium level (100 µs), pulse-off time at a low level (15 µs), powder concentration at a high level (4 g/l), and gain at a low level (0.83 mm/s) produced the best MRR. Authors in [13] investigated the PM-EDM of Ti–35Nb–7Ta–5Zr β-titanium alloy. When 4 g/l of Si powder were added to the dielectric fluid, there was a substantial drop in the density of surface cracks. A longer pulse interval and 8 g/l amount of Si powder particles were used to modify the β-Ti alloy. This resulted in interconnected surface porosities with pore sizes ranging from 200 to 500 nm. Additionally, the Recast Layer Thickness (RLT) was 8 µm and 2-3 µm for Si powder amounts of 2 g/l and 4 g/l, respectively. Furthermore, PM-EDM also enhanced the machining performance by improving the MRR and reducing the TWR. Authors in [14] explored the effect of nano alumina (Al_2O_3) powder added to the dielectric liquid and process parameters optimization deploying the Taguchi approach. The proposed nano Al_2O_3 mixed dielectric fluid gave increased MRR and reduced TWR and SR of the P20 steel workpiece. Authors in [15] examined how MRR, TWR, and Ra were affected by process variables including peak current, pulse duration, and powder percentage while machining high-speed steel (HSS)/(M2). In this study, the dielectric media are a mixture of SiC and graphite particles in equal proportions to transformer oil. It was discovered that, under different circumstances, adding graphite-SiC mixture powder to the dielectric fluid increased MRR and decreased Ra and TWR. I_P of 24 A, pulse duration of 100 µs, and powder concentration of 10 g/l yielded the highest MRR of 0.492 g/min. Also, 10 A, 100 µs, and 10 g/l produced the lowest TWR of 0.00126 g/min and 10 A, 50 µs, and 10 g/l produced optimized Ra of 3.51 µm.

It is concluded from the literature review that limited studies are available regarding nano Si or Ag powder mixed dielectric fluid and its process parameters optimization for any alloy. Also, there are no studies dealing with the effect of the PM-EDM process and its parameters on the Ti-35Nb-7Zr-5Ta alloy using Ag or Si powders. In this work, a deep investigation is performed to study the effect of pulse current, pulse-on, pulse-off, powder type (Ag, Si, and Ag+Si), and powder concentration on the MRR, and SR of Ti-35Nb-7Zr-5Ta and optimization adopting the Taguchi method combined with the Gray Relational Analysis (GRA).

II. EXPERIMENTAL PROCEDURES

A. Materials and Methods

All basic powders were imported from Sigma-Aldrich company. The powders were subjected to chemical composition analysis (by X-RF model Philips PW1480) and particle size analysis (by laser particle size analyzer model Bettersize 2000). The primary materials utilized in this research and their characteristics are displayed in Table I.

TABLE I. MATERIALS UTILIZED IN THIS RESEARCH AND THEIR CHARACTERISTICS

Material	Specifications
Ti powder	Purity: 99.990% Average particle size: 25.16 µm
Nb powder	Purity: 99.991% Average particle size: 5.072 µm
Ta powder	Purity: 99.990% Average particle size: 18.44 µm
Zr powder	Purity: 99.992% Average particle size: 11.39 µm
Ag powder	Purity: 99.997% Average particle size: 424 nm
Si powder	Purity: 99.996% Average particle size: 557nm
CP-Ti rod	Purity: 99.46%

The Ti-35Nb-7Zr-5Ta was prepared with the powder metallurgy technique. The powders were firstly weighed and mixed for 6 h putting into service an electric ball mixer, then, they were compacted using different compacting pressures, and the final pressure after which the green density was not substantially changed was 800 MPa. So, 800 MPa for 4 min was applied to compact all specimens in this study according to the green density stability under this pressure. Then, the green compacts were sintered in an electrical tubular resistance furnace employing Argon as the inert gas. The tube furnace heats up at a rate of 10 °C/min. To completely purge the alumina tube from the air during the 1st min of the sintering process, Argon atmosphere was exploited with 1.5 bar/min. For the subsequent minutes, 0.5 bar/min was engaged. This procedure involves raising the furnace temperature from room temperature to 500 °C for 2 h, 1300 °C for 16 h, and then slowly decreasing the temperature to room temperature. The sintered specimens were heat treated at 750 °C for 1 h,

followed by slow cooling inside the furnace. This treatment was conducted to increase the β-phase percentage, thus enhancing the biocompatibility of the resulting TNZT alloy. It can be noticed that the α-phase appears at angles 40.1° and 53.0° according to the card (JCPDS Card No. 06-0694), while the β-phase appears at angles 38.4°, 55.5°, and 69.6° according to the card (JCPDS Card No. 33-0397). The β-phase percentage was augmented, and the α-phase diminished as portrayed in Figure 1, where the α-phase decreased (according to the Pawly fit method) from 32.65% to 14.57% and the β-phase rose from 67.35% to 85.43% after the heat treatment process.

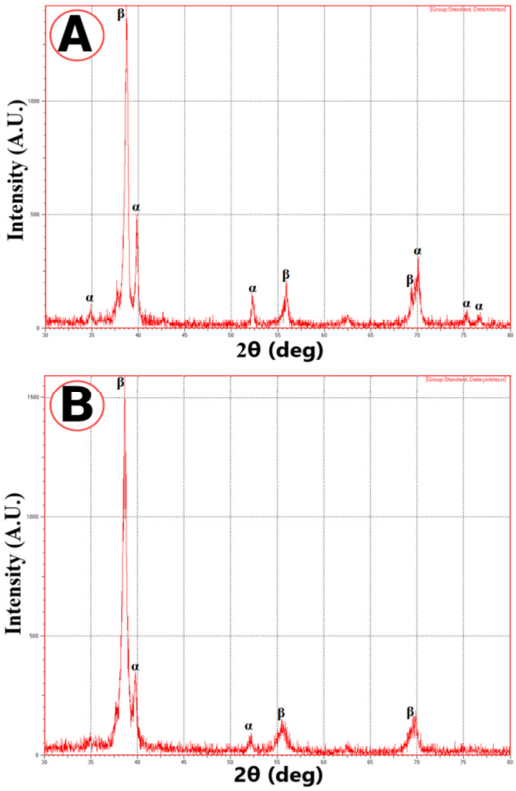

Fig. 1. XRD pattern for: (A) Sintered specimen, (B) sintered-heat-treated specimen.

These variations occurred because of the enough time given for the α-phase to transfer to the β-phase at this temperature. This result is in agreement with [16]. The specific heat treatment has a substantial effect on the mechanical properties of the TNZT implants. The increment of β-phase percentage means a lower elastic modulus, and when the elastic modulus of the implant is close to that of natural bone, the stress shielding phenomenon will be avoided. Also, the increment of β-phase percentage has a positive effect on implant hardness, as β-phase has higher hardness than α-phase.

B. PM-EDM Operation

The experiments were conducted on the Electric Discharge Machine model (CM 323C CHMER). In order to succeed in the experiments using powder mixed with dielectric fluid (Powder Mixed Electrical Discharge Machining PM-EDM), a small specially designed tank was deployed instead of the machine tank to prevent powder suspension in the original tank filter and to reduce the used powder quantity. The newly designed tank has a circulating pump with an arm to direct the powder-mixed dielectric fluid to the electrode-workpiece region. Also, an external stirrer was utilized to prevent powder accumulation in the bottom of the tank. Figure 2 depicts the experimental setup for the PM-EDM operation.

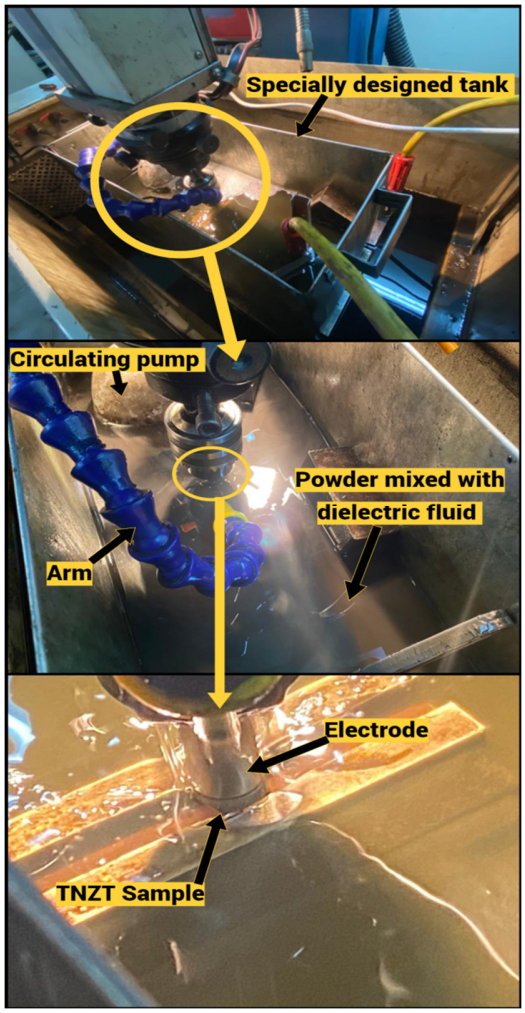

Fig. 2. Experimental setup for the PM-EDM operation used in this study.

The tool electrode is a cylinder-shaped, commercially pure Ti (grad 2) rod with a diameter of 12 mm. Eight lt of the dielectric fluid were placed in the machining container, and the hydrocarbon oil type HEDMA111 was utilized as dielectric fluid. In this study, additives of Ag or Si powders, or a mixture of both Ag (50%) and Si (50%) were applied in the dielectric fluid. The top and bottom surfaces of the Ti-35Nb-7Zr-5Ta specimen were ground to make a well-leveled surface finish.

In this paper the effect of powder mixed with dielectric fluid on MRR, and SR will be studied using different machining parameters, such as pulse current, pulse on, and pulse off. Table II provides the factors that were examined along with their levels.

TABLE II. CONTROL FACTORS AND THEIR LEVELS

Parameter	Designation	Unit	Levels		
			1	2	3
Pulse current	I	A	5	10	16
Pulse on	T_{on}	µs	9	18	37
Pulse off	T_{off}	µs	18	37	75
Powder type	P_T	/	Si	Ag	Ag+Si
Powder concentration	P_C	g/L	0	10	20

Five 3-level elements make up the current experiment arrangement. These levels were selected based on preliminary research, literature review, and machine capability. Other parameters that were kept constant during the experiment were the electrode (CP-grade II Ti), polarity (tool + and workpiece -), and duty cycle (8%). Taguchi orthogonal array of L27 (3^5) was selected. The array is observed in Table III. During machining, an external mixer was used to prevent powder sedimentation.

TABLE III. DESIGN OF EXPERIMENTS AND RESULTS OF METAL REMOVAL RATE AND SURFACE ROUGHNESS

No.	I	T_{on}	T_{off}	P_T	P_C	MRR (mm^3/min)	SR (µm)
1	1	1	1	1	1	0.8148	2.167
2	1	1	1	1	2	2.6943	1.849
3	1	1	1	1	3	7.0132	1.558
4	1	2	2	2	1	0.8452	2.289
5	1	2	2	2	2	4.244	1.604
6	1	2	2	2	3	8.9767	1.133
7	1	3	3	3	1	1.0679	2.591
8	1	3	3	3	2	3.5125	1.831
9	1	3	3	3	3	8.3148	1.388
10	2	1	2	3	1	7.1975	3.678
11	2	1	2	3	2	8.8651	3.219
12	2	1	2	3	3	10.4438	2.771
13	2	2	3	1	1	7.2133	3.885
14	2	2	3	1	2	9.3347	3.454
15	2	2	3	1	3	10.4268	3.141
16	2	3	1	2	1	8.9832	4.132
17	2	3	1	2	2	9.9542	3.572
18	2	3	1	2	3	12.63277	2.861
19	3	1	3	2	1	10.0883	4.722
20	3	1	3	2	2	14.3791	4.224
21	3	1	3	2	3	17.0354	3.577
22	3	2	1	3	1	11.2438	4.829
23	3	2	1	3	2	12.8887	4.586
24	3	2	1	3	3	14.6569	4.102
25	3	3	2	1	1	10.9012	4.931
26	3	3	2	1	2	11.8951	4.701
27	3	3	2	1	3	13.6742	4.495

III. RESPONSE FACTORS MEASUREMENT

The MRR is calculated with (1), while the (Ra) was measured with an Atomic Force Microscope (AFM) device model CSPM-AA3000.

$$MRR = \frac{W_i - W_f}{t \cdot \rho} \quad (1)$$

where W_i is the initial weight before machining (g), W_f is the final weight after machining (g), t is the machining time (min), and ρ represents workpiece density (g/mm^3).

IV. RESULTS & DISCUSSION

The results of the MRR, and SR for each of the 27 trials and their conditions are given in Table III.

A. MRR Result Analysis

In the PM-EDM process, more MRR provides an indicator for better machining performance. So, the MRR is considered the larger and the better criterion. The response value for the S/N ratio and the response value for means of MRR are exhibited in Table IV.

TABLE IV. RESPONSE VALUE FOR SIGNAL TO NOISE RATIOS AND FOR MEAN MRR VALUES

Response Value for S/N Ratios					
Level	Pulse current (A)	Pulse duration (µs)	Pulse off (µs)	Powder type	Powder amount (g/L)
1	9.309	16.453	16.817	16.183	12.506
2	19.385	17.070	16.845	17.675	17.473
3	22.153	17.324	17.185	16.989	20.868
Delta	12.843	0.870	0.368	1.491	8.363
Rank	1	4	5	3	2
Response Value for Means					
1	4.165	8.726	8.987	8.219	6.484
2	9.450	8.870	8.560	9.682	8.641
3	12.974	8.993	9.041	8.688	11.464
Delta	8.809	0.267	0.481	1.463	4.980
Rank	1	5	4	3	2

Higher spark energy corresponds to a higher current. Higher spark energy emerges from a rise in the pulse current, which generates a powerful spark that raises the temperature and causes the material to melt and vaporize as well as to form craters on the workpiece. This process produces greater material removal from the surface [17]. Hence, MRR increased with increasing pulse current. The maximum MRR value is 17.03 mm^3/min at the highest I of 16 A. A high pulse on time (pulse duration) indicates a longer period of sparking. As a result, material removal takes longer, and MRR rises with an increase in pulse duration. The rise in pulse duration might potentially increase the amount of electrons that strike the specimen, leading to a greater amount of material eroding off the workpiece surface per spark discharge [18]. Pulse interval (T_{off}) influences the speed and stability of the cut. In theory, the shorter interval leads to faster machining operation. When T_{off} increases, MRR first drops until it reaches halfway (T_{off} = 37 µs), at which point it begins to rise as T_{off} rises. The cause is that when T_{off} is short (up to 37 µs), there is a high chance of arcing, which prevents the dielectric fluid in the discharge gap from adequately flushing far away and leaves debris in the cutting gap. This generates arcing, which in turn leads to a fall in MRR. Better debris flushing occurs in the gap between the electrode and the workpiece when T_{off} increases after 37 µs, impeding arcing in the area where the MRR rises as T_{off} increases. This behavior of machining parameters is in accordance with the findings in [19].

MRR also rose with rising powder percentage in the hydrocarbon-based dielectric fluid [20]. This phenomenon occurred as a consequence of the spark gap growing when powder particles were added between the electrodes. Because of this, a greater number of charged powder particles filled the

space between the tool electrode and the workpiece, distributing the spark between the powder particles and the electrodes and augmenting the frequency and location of sparks [21]. This rise may be explained by the fact that the addition of powder lowers dielectric resistance, which causes the machining gap to grow and improves flushing conditions. Better spark ignition is simultaneously made possible by the powder particles that are present in the discharge gap. Thus, there are more pulses, which is the main factor contributing to the MRR enhancement [22]. Since the electrical conductivity of Ag powder ($6.3*10^7$ S/m) is higher than that of the Si powder ($4.35*10^{-4}$ S/m) and the electrical resistivity of Ag powder ($1.59*10^{-8}$ Ω·m) is less than that of the Si powder ($2.3*10^3$ Ω·m), this fact increases the sparking frequency by enabling sparking to occur at a greater distance than other particles. Additionally, because of the wider spark gap, debris is fast and easily washed away. Also, the thermal conductivity of Ag powder (429 W/m.K) is greater than that of Si powder (148 W/m.K), so more energy was transferred to the workpiece. MRR is enhanced more during the use of Ag powder than during the utilization of Si powder. On the other hand, the lower density of the Si powder (2.33 g/cm^3) than that of the Ag powder (10.49 g/cm^3) allows the former to easily mix with the dielectric resulting in MRR a bit lower than the one acquired when using the Ag powder. So, the maximum MRR value is 17.03 mm^3/min and emerged when adding 20 g/L Ag powder to the dielectric fluid. These findings are in accordance with the findings in [23]. The most important control factors that affect MRR can be concluded from Table IV. Pulse current occupies the first place, powder amount took the second place, while powder type, pulse off, and pulse on took the third, fourth, and fifth place, respectively. The contribution percentage of each control factor in controlling MRR can be determined by the ANOVA analysis. The contribution percentages are: 71%, 22.65%, 2%, 1.5%, and 1.35% for pulse current, powder amount, powder type, pulse-off, and pulse duration, correspondingly.

B. SR Analysis Results

In the PM-EDM process, low surface roughness provides an indicator for better machining performance. So, SR is considered the smaller the better criterion. The response value for the S/N ratio and the response value for means of MRR are demonstrated in Table V.

TABLE V. RESPONSE VALUE FOR SIGNAL TO NOISE RATIOS AND FOR MEAN SR VALUES

Response value for S/N ratios					
Level	**Pulse current (A)**	**Pulse duration (μs)**	**Pulse off (μs)**	**Powder type**	**Powder amount (g/L)**
1	-4.962	-9.255	-9.732	-9.862	-10.958
2	-10.592	-9.338	-9.229	-9.107	-9.540
3	-12.954	-9.916	-9.548	-9.540	-8.010
Delta	7.992	0.661	0.503	0.755	2.948
Rank	1	4	5	3	2
Response value for means					
1	1.823	3.085	3.295	3.353	3.692
2	3.413	3.225	3.202	3.124	3.227
3	4.463	3.389	3.201	3.222	2.781
Delta	2.640	0.304	0.094	0.230	0.911
Rank	1	3	5	4	2

As the pulse current rises, SR equivalently rises,. This happens because as the pulse current increased, a massive quantity of heat energy was created, which greatly melted the workpiece surface and caused surface damage. Explosions and the creation of gas bubbles were produced by the molten material being heated more, and thus, larger and deeper craters were formed increasing the SR value [24]. The surface roughness grows with the pulse duration, which goes from 9 to 37 μs. The discharge energy, that rises with an increase in the pulse duration, has the greatest impact on surface roughness. The size of the spark crater determines the surface roughness. A greater diameter and a shallower crater result in a smoother surface on the workpiece. By reducing the pulse-on time, it is crucial to regulate the electrical discharging energy at a lower level in order to get a flat crater. A huge discharge energy will generate strong sparks and a deeper surface erosion crater. As the molten metal cools down upon spilling, remnants will stay at the crater's periphery, creating a rough surface. Moreover, a larger crater established owing to increased discharge energy will result in a higher surface roughness value on the workpiece [25]. As the pulse-off time increases, the discharge energy drops. Moreover, the roughness diminishes in combination with the discharge energy. Also, proper flushing with augmented pulse-off time reduces the tendency of hot chips to get welded on the crater. So, surface roughness decreases with increasing pulse-off time [26].

The addition of powder particles in PM-EDM makes the insulating strength of the dielectric fluid decrease, increasing the spark-gap distance between the tool and the workpiece. The process becomes considerably more stable and the surface smoothness is enhanced due to the larger spark gap distance, which also makes uniform debris flushing easier. Consequently, the addition of powders to the dielectric fluid considerably ameliorates surface quality [11]. Moreover, when the discharge gap widens due to the addition of powder, less material—in the form of micro debris—is removed from the workpiece surface and less heat energy is produced. Micro-sized craters were thus created, improving surface smoothness [27]. Furthermore, the Ag powder mixed dielectric outperformed the Si powder mixed dielectric in terms of surface roughness. Since Ag is more conductive than Si, the machined surface experiences a uniform distribution of heat due to the increased gap distance and conductivity of the dielectric fluid. Additionally, given that the Ag particles are smaller (424 nm) and therefore penetrate the electrode gap in higher numbers, the overall discharge energy is dispersed more evenly across a wider surface, leading to the formation of several smaller craters during a single discharge [28]. So, the use of Ag powder particles has, therefore, produced better surface quality than that produced by the utilization of Si particles.

From Table V, the most important control factors that affect SR can be concluded. Pulse current occupied the first place, powder amount took the second place, while powder type, pulse on, and pulse off took the third, fourth, and fifth place, respectively. The contribution percentage of each control factor in controlling SR can be determined by ANOVA analysis. The contribution percentages are: 70.40%, 14.34%, 7.66%, 3.86%,

and 2.87% for pulse current, powder amount, powder type, pulse duration, and pulse-off, accordingly.

C. Optimization using Gray Relational Analysis (GRA)

1) Optimization of PM-EDM Process Parameters using GRA

GRA is a multi-response optimization technique, employed in the current study to determine the set of ideal parameters that provide the best MRR and surface finish. All results for (Grey Relational Coefficients) GRC and Grey Relational Grade (GRG) with their ranks are listed in Table VI.

TABLE VI. GRC AND GRG RESULTS

No.	GRC		GRG (γ_i)	Rank
	MRR $\xi_i(1)$	SR $\xi_i(2)$		
1	0.333	0.647	0.4904	15
2	0.361	0.726	0.5437	11
3	0.447	0.817	0.6322	4
4	0.334	0.622	0.4777	20
5	0.388	0.801	0.5946	5
6	0.502	1.000	0.7508	1
7	0.337	0.566	0.4513	22
8	0.375	0.731	0.5531	9
9	0.482	0.882	0.6817	3
10	0.452	0.427	0.4396	26
11	0.498	0.477	0.4873	16
12	0.552	0.537	0.5443	10
13	0.452	0.408	0.4303	27
14	0.513	0.450	0.4815	18
15	0.551	0.486	0.5185	13
16	0.502	0.388	0.4448	24
17	0.534	0.438	0.4858	17
18	0.648	0.524	0.5859	6
19	0.539	0.346	0.4423	25
20	0.753	0.381	0.5669	8
21	1.000	0.437	0.7186	2
22	0.583	0.339	0.4614	21
23	0.662	0.355	0.5083	14
24	0.773	0.390	0.5817	7
25	0.569	0.333	0.4513	23
26	0.612	0.347	0.4797	19
27	0.707	0.361	0.5340	12

If the relevant experimental result is closer to the ideal normalized value, the GRG is greater. Experiment No. 6 has the greatest multiple performance characteristics due to its highest GRG, so the combination of process variables of experiment No.6 is very close to the optimum parameters level. Referring to the response table of GRG (Table VII) and the response graph of means for GRG (Figure 3), the optimal parameter combination that maximizes overall response can be judged. The red line in Figure 3 represents the average GRG (0.531) of the 27 experiments.

TABLE VII. RESPONSE TABLE FOR MEAN GRG

Control Factors	GRG			Main effect	Rank
	Level 1	Level 2	Level 3		
Pulse current (A)	0.5751	0.4909	0.5271	0.084	2
Pulse duration (µs)	0.5406	0.5338	0.5186	0.022	4
Pulse off (µs)	0.5260	0.5384	0.5382	0.012	5
Powder type	0.5068	0.5630	0.5231	0.056	3
Powder amount (g/L)	0.4543	0.5223	0.6164	0.162	1

Maximum GRG exists at (I_1 T_{on1} T_{off2} P_{T2} P_{C3}). So, these conditions represent the optimal conditions for PM-EDM of the Ti-35Nb-7Zr-5Ta alloy to give maximum MRR with minimum SR. Also, the most important control factors that affect GRG can be concluded. Powder amount occupies the first place, pulse current takes the second place, while powder type, pulse duration, and pulse off take the third, fourth, and fifth place, respectively.

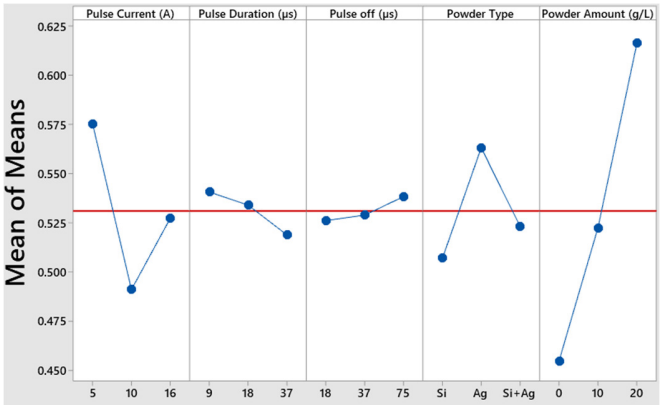

Fig. 3. Main effect plot for means of GRG.

2) Confirmation of the Optimum Results

An essential step in validating the optimal conditions that emerged from GRA is the confirmation experiment. This may be accomplished by experimentally applying the control factors' optimal conditions to get the response values (MRR and SR) under these conditions. Table VIII exhibits the results of the response factors employing the optimal conditions of the control factors.

TABLE VIII. CONFIRMATION TEST RESULTS

Response	Optimal conditions	Experimental results
MRR (mm³/min)	I_1 T_{on1} T_{off2} P_{T2} P_{C3}	8.5397
SR (µm)		1.093

The confirmation test results are close to the findings of the experiment No.6, with some changes, which derive from utilizing T_{on1} instead of T_{on2} in this experiment. Hence, the experimental result confirms the optimization of MRR and SR by deploying the GRA.

V. CONCLUSIONS

Ti-35Nb-7Zr-5Ta quaternary bio alloy fabricated by the powder metallurgy method was machined by Powder-Mixed Electrical Discharge Machining (PM-EDM) under different conditions. The following results were obtained:

1. Ti-35Nb-5Ta-7Zr alloy can be efficiently fabricated by powder metallurgy using 800 MPa compacting pressure and 18 h of sintering time (2 h at 500 °C and 16 h at 1300 °C).
2. The β-phase in the TNZT sample can be successfully increased by heat treatment at 750 °C for 1 h, where the α-phase decreased from 32.65% to 14.57% and the β-phase

increased from 67.35% to 85.43% after the heat treatment process. This phase is favorable in Ti-alloys due to its low elastic modulus, so, the stress shielding phenomenon can be avoided.

3. The addition of Ag, Si, or Ag+Si powders to the dielectric fluid enhances the metal removal rate and surface finish for the Ti-35Nb-5Ta-7Zr alloy.
4. The addition of Ag powder to the dielectric fluid gives higher MRR and lower SR compared to Si powder or Ag+Si.
5. Powder concentration and pulse current are the most effective parameters on MRR and SR followed by powder type, pulse-on, and pulse-off.
6. Maximum GRG exists at (I = 5 A, T_{on} = 9 µs, T_{off} = 37 µs, P_T = Ag, P_C = 20 g/L). So, these conditions represent the optimal conditions for PM-EDM of the Ti-35Nb-7Zr-5Ta alloy to give maximum MRR with minimum SR.

ACKNOWLEDGMENT

The authors thank all the staff of the Materials Engineering College, Metallurgical Engineering Department, University of Babylon, Iraq for their persistent assistance during the experimentation processes of this research.

REFERENCES

[1] N. V. Cuong and N. L. Khanh, "Parameter Selection to Ensure Multi-Criteria Optimization of the Taguchi Method Combined with the Data Envelopment Analysis-based Ranking Method when Milling SCM440 Steel," *Engineering, Technology & Applied Science Research*, vol. 11, no. 5, pp. 7551–7557, Oct. 2021, https://doi.org/10.48084/etasr.4315.

[2] V. C. Nguyen, T. D. Nguyen, and D. H. Tien, "Cutting Parameter Optimization in Finishing Milling of Ti-6Al-4V Titanium Alloy under MQL Condition using TOPSIS and ANOVA Analysis," *Engineering, Technology & Applied Science Research*, vol. 11, no. 1, pp. 6775–6780, Feb. 2021, https://doi.org/10.48084/etasr.4015.

[3] H. El-Hofy, *Advanced Machining Processes: Nontraditional and Hybrid Machining Processes*, 1st ed. New York, NY, USA: McGraw Hill, 2005.

[4] P. C. Pandey, *Modern MacHining Processes*, First Edition. New Delhi ; New York: McGraw-Hill, 1981.

[5] P. C. Pandey, *Modern MacHining Processes*, 1st ed. New Delhi, India ; New York, NY, USA: McGraw-Hill, 1981.

[6] S. Anjum, M. Shah, N. A. Anjum, S. Mehmood, and W. Anwar, "Machining and Surface Characteristics of AISI 304L After Electric Discharge Machining for Copper and Graphite Electrodes in Different Dielectric Liquids," *Engineering, Technology & Applied Science Research*, vol. 7, no. 4, pp. 1765–1770, Aug. 2017, https://doi.org/10.48084/etasr.1250.

[7] S. Anjum, M. Shah, N. A. Anjum, S. Mehmood, and W. Anwar, "Machining and Surface Characteristics of AISI 304L After Electric Discharge Machining for Copper and Graphite Electrodes in Different Dielectric Liquids," *Engineering, Technology & Applied Science Research*, vol. 7, no. 4, pp. 1765–1770, Aug. 2017, https://doi.org/10.48084/etasr.1250.

[8] D. Kumar, V. Kumar Pathak, and R. Singh, "Effect of powder mixed dielectric medium in electrical discharge machining – A review," *Materials Today: Proceedings*, vol. 62, pp. 1596–1600, Jan. 2022, https://doi.org/10.1016/j.matpr.2022.03.391.

[9] T. Muthuramalingam and B. Mohan, "A review on influence of electrical process parameters in EDM process," *Archives of Civil and Mechanical Engineering*, vol. 15, no. 1, pp. 87–94, Jan. 2015, https://doi.org/10.1016/j.acme.2014.02.009.

[10] K. Ojha, R. K. Garg, and K. K. Singh, "MRR Improvement in Sinking Electrical Discharge Machining: A Review," *Journal of Minerals and Materials Characterization and Engineering*, vol. 9, no. 8, pp. 709–739, 2010, https://doi.org/10.4236/jmmce.2010.98051.

[11] A. Y. Joshi and A. Y. Joshi, "Multi response optimization of PMEDM of Ti6Al4V using Al2O3 and SiC powder added de-ionized water as dielectric medium using grey relational analysis," *SN Applied Sciences*, vol. 3, no. 7, Jun. 2021, Art. no. 718, https://doi.org/10.1007/s42452-021-04712-3.

[12] H. K. Kansal, S. Singh, and P. Kumar, "Effect of Silicon Powder Mixed EDM on Machining Rate of AISI D2 Die Steel," *Journal of Manufacturing Processes*, vol. 9, no. 1, pp. 13–22, Jan. 2007, https://doi.org/10.1016/S1526-6125(07)70104-4.

[13] C. Prakash, H. K. Kansal, B. S. Pabla, and S. Puri, "Experimental investigations in powder mixed electric discharge machining of Ti–35Nb–7Ta–5Zrβ-titanium alloy," *Materials and Manufacturing Processes*, vol. 32, no. 3, pp. 274–285, Feb. 2017, https://doi.org/10.1080/10426914.2016.1198018.

[14] M.- Ashok, T. Niranjan, S. Chokalingam, and B. Singaravel, "Investigation of powder mixed electrical discharge machining and process parameters optimization using Taguchi based overall evaluation criteria," *IOP Conference Series: Materials Science and Engineering*, vol. 1057, no. 1, Oct. 2021, Art. no. 012075, https://doi.org/10.1088/1757-899X/1057/1/012075.

[15] S. R. Fadhil and S. H. Aghdeab, "Effect of Powder-Mixed Dielectric on EDM Process Performance," *Engineering and Technology Journal*, vol. 38, no. 8A, pp. 1226–1235, Aug. 2020, https://doi.org/10.30684/etj.v38i8A.554.

[16] M. Hein *et al.*, "Heat Treatments of Metastable β Titanium Alloy Ti-24Nb-4Zr-8Sn Processed by Laser Powder Bed Fusion," *Materials*, vol. 15, no. 11, Jan. 2022, Art. no. 3774, https://doi.org/10.3390/ma15113774.

[17] D. Doreswamy, D. S. Shreyas, S. K. Bhat, and R. N. Rao, "Optimization of material removal rate and surface characterization of wire electric discharge machined Ti-6Al-4V alloy by response surface method," *Manufacturing Review*, vol. 9, 2022, Art. no. 15, https://doi.org/10.1051/mfreview/2022016.

[18] M. Bhaumik and K. Maity, "Effect of different tool materials during EDM performance of titanium grade 6 alloy," *Engineering Science and Technology, an International Journal*, vol. 21, no. 3, pp. 507–516, Jun. 2018, https://doi.org/10.1016/j.jestch.2018.04.018.

[19] S. H. Aghdeab and A. I. Ahmed, "Effect of Pulse on Time and Pulse off Time on Material Removal Rate and Electrode Wear Ratio of Stainless Steel AISI 316L in EDM," *Engineering and Technology Journal*, vol. 34, no. 15A, pp. 2940–2949, Dec. 2016, https://doi.org/10.30684/etj.34.15A.14.

[20] A. Sugunakar, A. Kumar, and R. Markandeya, "Effect of Powder Mixed Dielectric fluid on Surface Integrity by Electrical Discharge Machining of RENE 80," *IOSR Journal of Mechanical and Civil Engineering*, vol. 14, no. 3, pp. 43–50, May 2017, https://doi.org/10.9790/1684-1403044350.

[21] A. Y. Joshi and A. Y. Joshi, "A systematic review on powder mixed electrical discharge machining," *Heliyon*, vol. 5, no. 12, Dec. 2019, https://doi.org/10.1016/j.heliyon.2019.e02963.

[22] B. Bhattacharyya and B. Doloi, "Chapter Six - Hybrid machining technology," in *Modern Machining Technology*, Cambridge, MA, USA: Academic Press, 2020, pp. 461–591.

[23] F. Klocke, D. Lung, G. Antonoglou, and D. Thomaidis, "The effects of powder suspended dielectrics on the thermal influenced zone by electrodischarge machining with small discharge energies," *Journal of Materials Processing Technology*, vol. 149, no. 1, pp. 191–197, Jun. 2004, https://doi.org/10.1016/j.jmatprotec.2003.10.036.

[24] Y.-F. Tzeng and C.-Y. Lee, "Effects of Powder Characteristics on Electrodischarge Machining Efficiency," *The International Journal of Advanced Manufacturing Technology*, vol. 17, no. 8, pp. 586–592, Apr. 2001, https://doi.org/10.1007/s001700170142.

[25] S. Singh and P. K. Sharma, "The Effect of Edm Parameters on Surface Roughness and Material Removal Rate," *International Journal of*

Technical Research & Science, vol. 3, no. 4, pp. 134–138, May 2018, https://doi.org/10.30780/IJTRS.V3.I3.2018.021.

[26] S. Banerjee, D. Mahapatro, and S. Dubey, "Some study on electrical discharge machining of ({WC+TiC+TaC/NbC}–Co) cemented carbide," *The International Journal of Advanced Manufacturing Technology*, vol. 43, no. 11, pp. 1177–1188, Aug. 2009, https://doi.org/10.1007/s00170-008-1796-7.

[27] B. Singh, J. Kumar, and S. Kumar, "Influences of Process Parameters on MRR Improvement in Simple and Powder-Mixed EDM of AA6061/10%SiC Composite," *Materials and Manufacturing Processes*, vol. 30, no. 3, pp. 303–312, Mar. 2015, https://doi.org/10.1080/10426914.2014.930888.

[28] K.-Y. Kung, J.-T. Horng, and K.-T. Chiang, "Material removal rate and electrode wear ratio study on the powder mixed electrical discharge machining of cobalt-bonded tungsten carbide," *The International Journal of Advanced Manufacturing Technology*, vol. 40, no. 1, pp. 95–104, Jan. 2009, https://doi.org/10.1007/s00170-007-1307-2.